Assessing the relationships between interdigital geometry quality and inkjet printing parameters

WCMNM 2021

Federico Bertolucci[1] Nicolò Berdozzi[1] Lara Rebaioli[2] Trunal Patil[2]
Rocco Vertechy[1] Irene Fassi[2]

[1]*University of Bologna, Industrial Engineering Department, Bologna, Italy*
[2]*Consiglio Nazionale delle Ricerche, Institute of Intelligent Industrial Technologies and Systems for Advanced Manufacturing, Milan, Italy*

Abstract

Drop on demand (DoD) inkjet printing is a high precision, non-contact and maskless additive manufacturing technique employed in producing high precision micrometer-scaled geometries allowing a free design manufacturing for flexible devices and printed electronics. This study investigates the influence of the main printing parameters (namely, the spacing between subsequent drops deposited on the substrate, the printing speed, and the nozzle temperature) on the dimensional accuracy of a representative geometry consisting of two interlocked comb shapes. The study objective was achieved thanks to a proper experimental campaign, which was developed according to Design of Experiments (DoE).

Keywords: Additive manufacturing, inkjet printing, interdigital geometry, image processing, Design of Experiment

1. Introduction

During the last decades, the combination of computer design and 3-dimensional printing technique took the workflow of manufacturing processes to a substantial change in several science fields such as biology, life science and robotics. In particular, inkjet printing has been widely used as high precision additive manufacturing technique to produce devices like transducers [1] and sensors [2].

Inkjet printing technology can be divided in two subcategories: continuous and drop on demand (DoD). In the former the creation of ink droplets is constant and allows to perform high speed printing process especially for industrial employment. In the latter, a single drop is ejected from the nozzle, allowing smaller drop size generation and higher placement accuracy [3]. Although other printing, coating, and casting processes such as screen printing, spin-coating, top-down etching, or blade casting are commonly used as they offer a low-cost and large covered area results [4], they involve the contact with the sample and often require the use of masks. DoD inkjet printing takes advantages of its contact-free, maskless, digitally controlled operating mode to design micrometer-scaled geometries. The possibility to create flexible electronics through DoD printing process gives access to a wide employment in applications such as microelectromechanical systems [5], dielectric elastomer transducers [6] and electro-adhesive devices [7]. All these applications need a high precision technology that works at the micrometer scale and a free geometry feasibility.

As emerged in past works [7], the result of the inkjet printing process strongly depends on the materials choice and on the interaction between ink and substrate. The literature shows a lot of studies regarding the delivery of the ink droplets from the nozzle to the substrate [8, 9], as well as the jet fluid dynamics [10, 11], but no systematic approaches exist dealing with the relationship between process parameters and geometrical outcome. Moreover, in literature there is no findings about an optimal set of parameters in the printing process, neither by using the statistical procedure of the Design of Experiment (DOE) [12].

This work proposes a methodology to set a suitable range for relevant printing parameters (i.e. the spacing between subsequent drops deposited on the substrate, the printing speed, and the nozzle temperature) with the aim of ensuring a good accuracy of the result. A geometry consisting of two interlocked comb shapes, commonly known as interdigital geometry, was chosen as representative example, since it requires precise printed lines spaced by a homogeneous gap. The study objective was achieved thanks to a proper experimental campaign, which was developed according to Design of Experiments (DoE).

2. Materials and methods

2.1. Geometry design and manufacturing

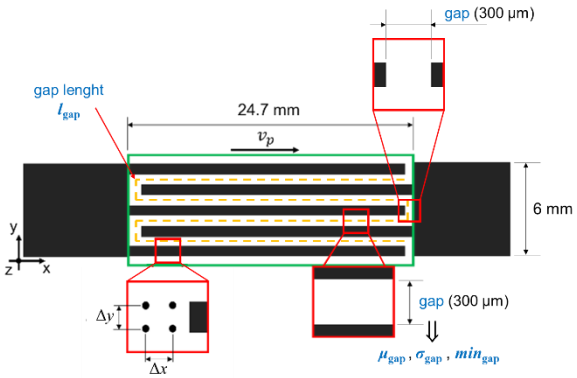

Fig. 1 Interdigital geometry

Two interdigital geometries are printed so that the comb-fingers are interposed one to each other. Fig. 1 shows the nominal dimensions of the selected reference geometry. The distance between two fingers is named hereafter as “gap”. The line describing the path within the fingers is named as “gap length”.

The MicroFab Jetlab 4xl printer with a 50 µm diameter piezoelectric nozzle is used for the ink deposition (Fig. 2a). An ink droplet is generated

through a pressure variation in the ink reservoir, induced by the vibration of a piezoelectric plate. The drop deposition reference system consists in an aluminum plate sliding horizontally on magnetic rails describing the x-y plane and in a z-axis referred to the motion of the printhead, perpendicular to the plate. A vacuum system allows to bond the substrate to the plate during the printing process. A heat control unit is connected both to the printhead and the plate driving separately the two temperature levels that are sensed by thermocouples.

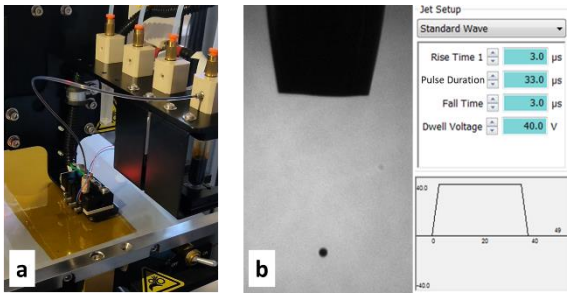

Fig. 2 a) MicroFab Jetlab 4xl printer; b) Stable drop and voltage waveform

The interdigital geometry is printed as a combination of several drop arrays. The printing direction corresponds to the main length of the array that is the x-direction.

A commercial conductive silver-nanoparticle ink (Smart 'Ink S-CS01130 from Genes 'Ink) is used to print due to the high ink stability for droplet formation, good reproducibility of the geometries and its low resistivity (around 15 µΩ/cm). The ink is prepared to be printed by filtering it with a 0,45 µm PTFE syringe filter and 5 minutes of ultrasonic bath to dissolve any particle aggregation. Once the geometry is printed, the ink is cured in oven at 150°C for 40 minutes.

A polyimide (PI) film 25.4 µm thick is used as substrate. The substrate is industrially produced in rolls by Caplinq (PIT1N/210), and it has been preferred to a custom realization to guarantee the uniformity of the substrate avoiding interference with the ink distribution in the printed pattern.

2.2. Experimental design

The effects of the selected parameters on the process performance were studied using a suitable experimental design (Table 1). The four selected factors are the printing speed along the x-axis, the subsequent drop spacing along the x-axis, the subsequent drop spacing along the y-axis, and the nozzle temperature.

The printer setup, involving the voltage waveform and the backpressure of printing channel, is adjusted to obtain a stable drop flight [13, 14, 15] and kept constant throughout the entire experimental design. A monopolar trapezoidal wave is set to the parameters shown in Fig. 2b. The reservoir pressure is set to -10 Pa, leading to a flat ink meniscus at the nozzle tip.

Two levels were selected for each factor based on preliminary experiments and in accordance with machine positioning tolerance (i.e. ± 30 µm in the x-y directions), thus resulting in $2^4 = 16$ different experimental conditions. Two replicates were carried out for each experimental condition while five replicates were carried out for the central point (v_p = 20 mm/s, Δx = 110 µm and Δy = 140 µm) at each temperature level. Therefore, the whole experimental design included 42 runs, which were completely randomized.

Table 1
Experimental design summary

Factor	Symbol	Levels	
		Low	High
x-axis spacing (µm)	Δx	80	140
y-axis spacing (µm)	Δy	110	170
Printing speed (mm/s)	v_p	10	30
Nozzle temperature (°C)	T_n	35	40

The responses that were analysed by means of the Analysis of Variance (ANOVA) are the mean value and standard deviation of the gap. Moreover, the minimum value of the gap and the gap length were observed to better assess the printing quality. The calculation of the responses is discussed in the following section.

2.3. Measurements and analysis

A Zeiss Stereo Discovery V20 optical microscope was used to acquire and measure the printed samples, then a MATLAB code was run to extract the geometrical parameters by using image processing algorithms.

The geometrical parameters to be evaluated (Fig. 1) are defined as follows:

- mean value of the gap (μ_{gap}): this parameter aims at evaluating the average magnitude of the gap;
- standard deviation of the gap (σ_{gap}): this parameter aims at evaluating the regularity of the gap along the shape;
- minimum value of the gap (min_{gap}): this parameter can highlight singularities in the contour lines, such as extra ink deposits, and interconnections between the arrays;
- gap length (l_{gap}): this parameter can show if there are some disconnections in the arrays.

Classical image process functions acquire features of the printed sample and calculate the Euclidean distance between distinct arrays. If the distance is lower than the threshold of 500 µm, the program calculates the mean value, standard deviation, and minimum value of the whole set of distances (μ_{gap}, σ_{gap} and min_{gap}, respectively). Only contiguous horizontal arrays represent optimal outcomes, so the ones disconnected from the thicker rectangles on the geometry sides are not considered in the gap calculation. The gap length l_{gap} corresponds to the number of pixels for which a gap distance is calculated, converted in millimeters.

3. Results and discussion

Suitable models were analyzed to study the effect of the factors listed in Table 1 on the mean value and standard deviation of the gap.

Table 2 summarizes the ANOVA results, showing the statistically significant factors, while the plots in Fig. 3, Fig. 4, Fig. 5, and Fig. 6 depict the results related to the mean value and standard deviation of the gap for each factor.

Table 2
ANOVA p-values (bold = significant factor, confidence level α = 5%) for the analysis on the mean value and standard deviation of the gap

Factors		**P-value**	
		μ_{gap}	σ_{gap}
Main factors	Δx	**0.000**	**0.001**
	Δy	**0.000**	**0.000**
	v_p	0.166	0.243
	T_n	**0.030**	0.199
Interactions	Δx*Δy	**0.000**	**0.043**
	Δx*v_p	0.088	0.405
	Δx*T_n	**0.043**	**0.003**
	Δy*v_p	0.769	**0.021**
	Δy*T_n	0.523	0.353
	v_p*T_n	0.721	0.201

Based on the ANOVA results resumed in Table 2, both responses are affected by the drop spacing along the X and the Y axes. As both factors increase, the mean size of the gap shows values that are higher and closer to the nominal value (300 µm), while the standard deviation decreases (Fig. 3 and Fig. 4).

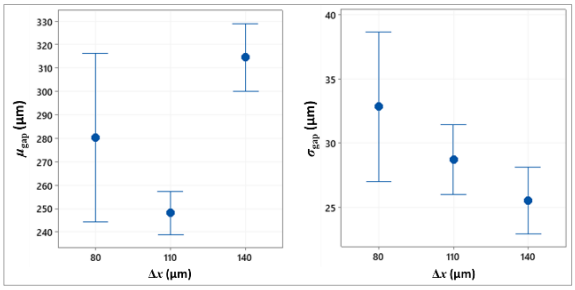

Fig. 3 Interval plot of the mean value and standard deviation of the gap against drop spacing along the x-axis

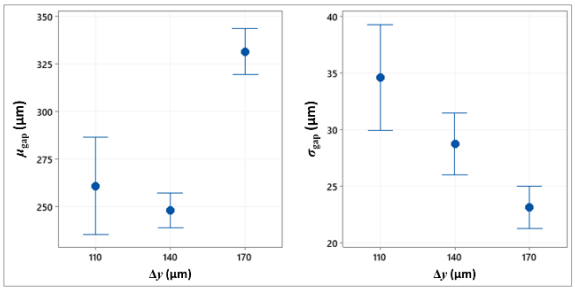

Fig. 4 Interval plot of the mean value and standard deviation of the gap against drop spacing along the y-axis

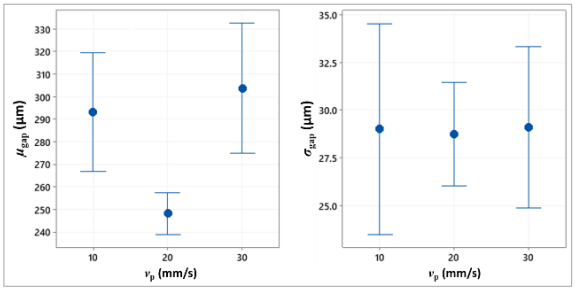

Fig. 5 Interval plot of the mean value and standard deviation of the gap against the printing speed

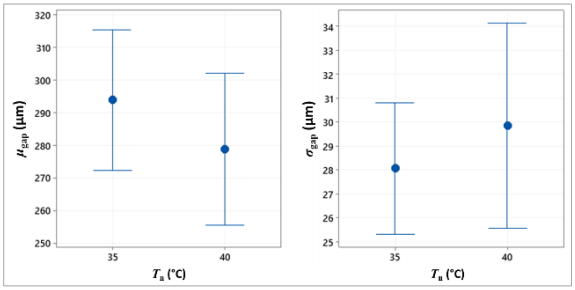

Fig. 6 Interval plot of the mean value and standard deviation of the gap against the nozzle temperature

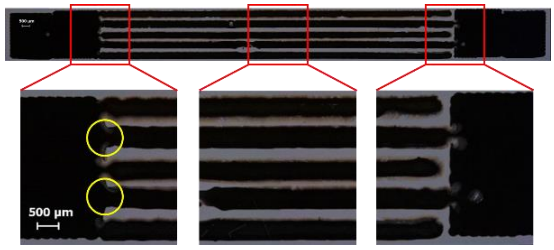

Fig. 7 Example of printed sample with interconnected arrays (Δx = 80 µm, Δy = 110 µm, v_p = 10 mm/s, T_n = 40°C)

A higher spacing between the subsequent drops, regardless of the direction, reduces the drop overlapping and, thus, the spreading of excess ink. Therefore, this allows to obtain lines that are less thick and more regular, helping to respect the target size and shape of the gap (σ_{gap} = 25.5 ± 4.9 µm at Δx = 140 µm and σ_{gap} = 23.2 ± 3.4 µm at Δy = 170 µm, as shown in Fig. 3 and Fig. 4). Conversely, lower spacing leads to undesired ink exceedances causing non-homogeneous boundaries, with consequent reduction of the gap mean value and increase of the gap standard deviation (e.g. in Fig. 7).

The nozzle temperature proved to affect the mean size of the gap, whose value decreases as the temperature increase (Fig. 6). This is probably caused by the dependence of ink viscosity from the temperature, which results in a higher ink spreading when the temperature increases.

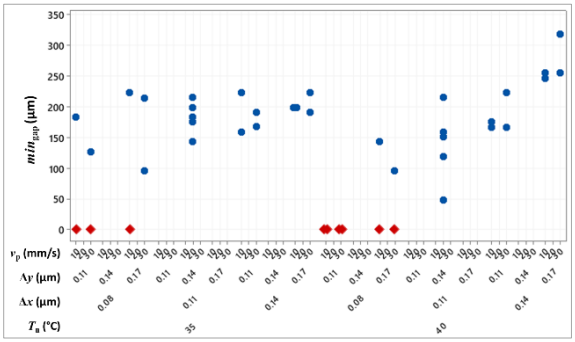

Fig. 8 Individual value plot of the minimum value of the gap

The minimum value of gap and the gap length proved to be helpful in identifying undesired conditions with respect to the nominal geometry.

Fig. 8 depicts the experimental results in terms of minimum value of the gap. It should be noticed that the majority of the experimental conditions with Δx = 80 µm resulted in a value of min_{gap} equal to zero (red diamonds in Fig. 8), meaning that the arrays are interconnected, as shown by yellow circles in Fig. 7, corrupting the geometry shape. Thus, all the process

parameter combinations including Δx = 80 µm are likely to be unsuitable.

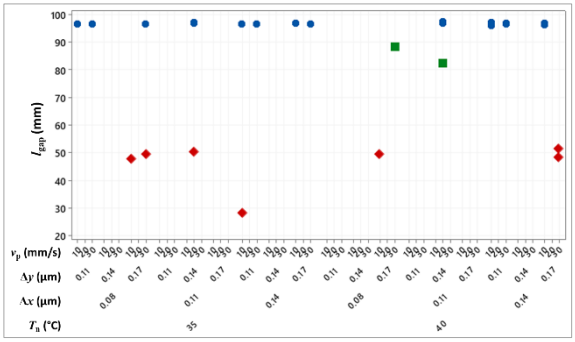

Fig. 9 Individual value plot of gap length

Fig. 9 shows the gap length that was measured for the samples that do not present interconnections. A gap length that is much lower than the nominal value (red diamonds in Fig. 9) implies that there are disconnections at the beginning of an array (Fig. 10a). A gap length that is slightly lower than the nominal value (green squares in Fig. 9) means that there is a disconnection at some intermediate point of an array (Fig. 10b). The experimental data do not exhibit clear relationships between the process parameters and the disconnections, which are likely to be caused by random issues, such as dust or ink-substrate anomalous interaction, due to substrate defects or ink aggregates.

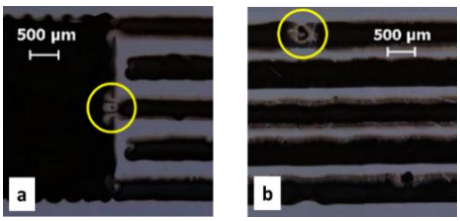

Fig. 10 a) Example of disconnection at the array beginning (Δx = 140 mm, Δy = 170 mm, v_p = 30 mm/s, T_n = 35°C); b) Example of intermediate disconnection (Δx = 110 mm, Δy = 140 mm, v_p = 20 mm/s, T_n = 40°C)

4. Conclusions

This study investigated the application of the DoD inkjet printing technology to the manufacturing of a micrometer-scaled representative geometry, i.e. the so-called interdigital geometry consisting of two interlocked comb shapes. A suitable experimental design was studied to assess the influence of the spacing between subsequent drops, the printing speed and the nozzle temperature on the process output.

The experimental results showed that the drop spacing along both the x-axis and the y-axis have an influence on the width and the regularity of the gap between the arrays. In particular, the spacing along the printing direction (x-axis) proved to be critical for avoiding interconnections between the arrays. Moreover, the results pointed out that the nozzle temperature affects the gap mean value. Eventually, the process output was also influenced by issues related to substrate damages or dust fibers. Therefore, performing the experimental campaign in a controlled environment could limit these issues.

This work allowed to create a repeatable methodology for assessing the relationships between geometrical quantities and printing parameters, which can be extended to other ink-substrate couples. The developed analysis tools could also be used in a quality check procedure for batch produced inkjet printed shapes.

Acknowledgements

This work was partially funded by the European Union under the DiManD project (H2020-MSCA-ITN, grant agreement No. 814078).

References

[1] B. Andò et al., “Low-cost inkjet printing technology for the rapid prototyping of transducers,” Sensors (Basel), 2017; 17 (4): 748.

[2] G. Mattana et al., “Recent advances in printed sensors on foil,” Mater. Today, 2016; 19 (2): 88-99.

[3] J. Li et al., “Inkjet printing for biosensor fabrication: Combining chemistry and technology for advanced manufacturing,” Lab Chip, 2015; 15 (12): 2538-2558.

[4] F.C. Krebs, “Fabrication and processing of polymer solar cells: A review of printing and coating techniques,” Sol. Energy Mater. Sol. Cells, 2009; 93 (4): 394-412.

[5] G.K. Lau et al., “Ink-jet printing of micro-elelectro-mechanical systems (MEMS),” Micromachines (Basel), 2017; 8 (6): 1-19.

[6] S. Schlatter et al., “Inkjet printing of carbon black electrodes for dielectric elastomer actuators,” Electroact. Polym. Actuators Devices, 2017; 10163: 1016311.

[7] N. Berdozzi et al., “Rapid Fabrication of Electro-Adhesive Devices with Inkjet Printed Electrodes,” IEEE Rob. Autom. Lett., 2020; 5 (2): 2770-2776.

[8] N. Reis et al., “Ink-jet delivery of particle suspensions by piezoelectric droplet ejectors,” J. Appl. Phys., 2005; 97: 094903.

[9] A.S. Yang et al., “Investigation of droplet-ejection characteristics for a piezoelectric inkjet printhead,” Proc. Inst. Mech. Eng., Part C: J. Mech. Eng. Sci., 2006; 220 (4): 435-444.

[10] B.W. Jo et al., “Evaluation of jet performance in drop-on-demand (DOD) inkjet printing,” Korean J. Chem. Eng., 2009; 26 (2): 339-348.

[11] G.D. Martin et al., “Inkjet printing - The physics of manipulating liquid jets and drops,” J. Phys. Conf. Ser., 2008; 105 (1): 012001.

[12] J. Abu-Khalaf et al., “Optimization of geometry parameters of inkjet-printed silver nanoparticle traces on PDMS substrates using response surface methodology,” Materials (Basel), 2019; 12 (20): 3329.

[13] S.D. Hoath et al., “Dependence of drop speed on nozzle diameter, viscosity and drive amplitude in drop-on-demand ink-jet printing,” Int. Conf. Digit. Print. Technol., 2011; 62-65.

[14] H. Dong et al., “An experimental study of drop-on-demand drop formation,” Phys. Fluids, 2006; 18 (7): 072102.

[15] B.K.L. Jiayan Tai et al., “Control of Droplet Formation in Inkjet Printing Using Ohnesorge Number Category: Materials and Processes Jiayan,” Electron. Packag. Technol. Conf., 2008.